Research in Astronomy and Astrophysics, 23:015007 (7pp), 2023 January https://doi.org/10.1088/1674-4527/aca233

Properties of the Main Phases of the Super Geomagnetic Storms (ΔSYM-H $\leqslant -250$ nT) with Different Heliolongitudes

Ming-Xian Zhao[1,2], Gui-Ming Le[1,2,3,4], and Yong-Hua Liu[1,5]

[1] Key Laboratory of Space Weather, National Satellite Meteorological Center (National Center for Space Weather), China Meteorological Administration, Beijing 100081, China; Legm@cma.gov.cn

[2] School of Physics Science & Technology, Lingnan Normal University, Zhanjiang 524048, China

[3] Innovation Center for FengYun Meteorological Satellite (FYSIC), Beijing 100081, China

[4] CAS Key Laboratory of Solar Activity, National Astronomical Observatories, Beijing 100101, China

[5] Polar Research Institute of China, Shanghai 200136, China

Received 2022 September 17; revised 2022 October 27; accepted 2022 November 9; published 2022 December 9

Abstract

We studied the properties of the main phases of 24 super geomagnetic storms (SGSs) (ΔSYM-H $\leqslant -250$ nT) since 1981. We divided the SGSs into two subgroups: SGSs-I (-400 nT $< \Delta$ SYM-H $\leqslant -250$ nT) and SGSs-II (ΔSYM-H $\leqslant -400$ nT). Of the 24 SGSs, 16 are SGSs-I and eight are SGSs-II. The source locations of SGSs were distributed in the longitudinal scope of [E37, W66]. 95.8% of the SGSs were distributed in the longitudinal scope of [E37, W20]. East and west hemispheres of the Sun had 14 and 10 SGSs, respectively. The durations of the main phases for six SGSs ranged from 2 to 4 hr. The durations of the main phases for the rest 18 SGSs were longer than 6.5 hr. The duration of the SGSs with source locations in the west hemisphere varied from 2.22 to 19.58 hr. The duration for the SGSs with the source locations in the east hemisphere ranged from 2.1 to 31.88 hr. The averaged duration of the main phases of the SGSs in the west and east hemispheres are 8.3 hr and 13.98 hr, respectively. $|\Delta\mathrm{SYM{-}H}/\Delta t|$ for six SGSs with source locations distributed in the longitudinal area ranging from E15 to W20 was larger than $1.0\,\mathrm{nT}\cdot\mathrm{minute}^{-1}$, while $|\Delta\mathrm{SYM{-}H}/\Delta t|$ for the rest 18 SGSs was lower than $1.0\,\mathrm{nT}\cdot\mathrm{minute}^{-1}$.$|\Delta\mathrm{SYM{-}H}/\Delta t|$ for SGSs-I varied from 0.18 to $3.0\,\mathrm{nT}\cdot\mathrm{minute}^{-1}$. $|\Delta\mathrm{SYM{-}H}/\Delta t|$ for eight SGSs-II varied from 0.37 to $2.2\,\mathrm{nT}\cdot\mathrm{minute}^{-1}$ with seven SGSs-II falling in the scope from 0.37 to $0.992\,\mathrm{nT}\cdot\mathrm{minute}^{-1}$.

Key words: The Sun – (Sun:) solar-terrestrial relations – (Sun:) solar wind

1. Introduction

Both Dst index and SYM-H index can be used to describe the intensity of a geomagnetic storm. However, the time resolution of SYM-H index is much higher than that of Dst index and can be treated as high time resolution of Dst index (Wanliss & Showalter 2006). Hence, only the SYM-H index can describe the rapid variation of the ring current although there is some difference between Dst index and SYM-H index (Katus & Liemohn 2013). It has been proved that the temporal variation of the solar wind parameters correlates well with that of the SYM-H index, but not with that of Dst index (Li et al. 2022). The variation of the SYM-H index during the main phase of a geomagnetic storm (hereafter ΔSYM-H) is usually different from the minimum of SYM-H ($\mathrm{SYM\text{-}H_{min}}$). A geomagnetic storm with Δ SYM-H $\leqslant -250$ nT is defined as a super geomagnetic storm (SGS) in this study. SGSs are the severe space weather phenomena because these kinds of geomagnetic storms may lead to widespread interference and damage to technological systems (Love 2021, and references therein) and then lead to significant economic loss (e.g., Council National Research 2008; Schulte in den Bäumen et al. 2014; Eastwood et al. 2017; Ganushkina et al. 2017; Riley & Love 2017).

Many articles have been devoted to the study of the solar and interplanetary sources for single or many SGSs that occurred during the period from 1957 to the present (e.g., Garcia & Dryer 1987; Allen et al. 1989; Cliver & Crooker 1993; Smart & Shea 1996; Huttunen et al. 2002; Gopalswamy et al. 2005a, 2005b, 2022; Farrugia et al. 2005; Jadav et al. 2005; Xue et al. 2005; Zhang et al. 2007; Kataoka & Miyoshi 2008; Cliver et al. 2009, 2022; Liu et al. 2014; Lugaz et al. 2015; Lefèvre et al. 2016; Vennerstrom et al. 2016; Wu et al. 2016; Riley et al. 2018; Meng et al. 2019; Cheng et al. 2020; Le & Zhao 2021a; Le et al. 2021b; Li et al. 2022). Many articles have also been devoted to the estimation of the intensities of geomagnetic storms (e.g., Burton et al. 1975; Murayama 1982; Fenrich & Luhmann 1998; O'Brien & McPherron 2000; Temerin & Li 2002; Wang et al. 2003b; Tsurutani et al. 2003; Kumar et al. 2015; Gopalswamy 2018; Zhao et al. 2022).

Properties of the main phase of an SGS we concerned are the time length of the main phase (Δt), the variation of the ring current during the main phase of an SGS, and the averaged increase speed of the ring current during the main phase of an

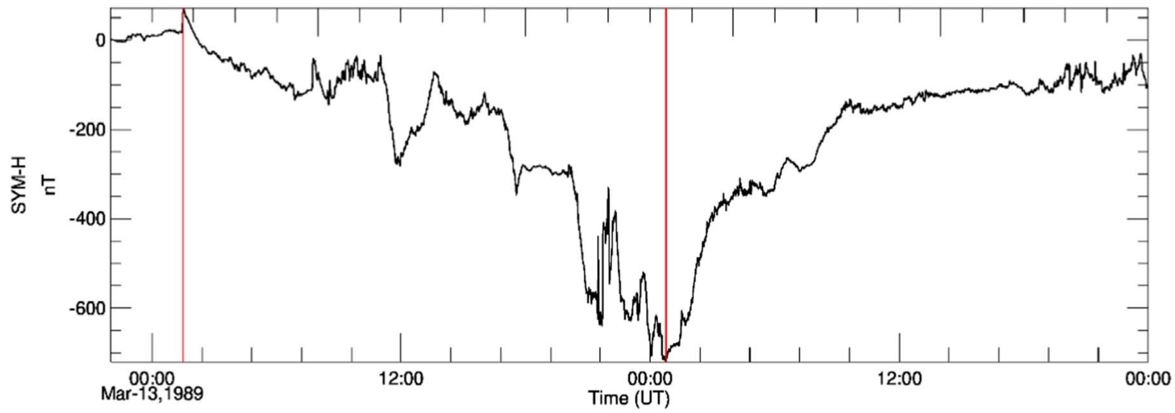

Figure 1. The properties of the main phase of the SGS that occurred during 1989 March 13–14.

SGS (ΔSYM$-$H$/\Delta t$). To investigate the properties of the SGSs with different intensities, the SGSs were divided into two subgroups: SGSs-I (-400 nT $<\Delta$ SYM-H $\leqslant -250$ nT) and SGSs-II (ΔSYM-H $\leqslant -400$ nT). Are these properties related to the source locations of the associated SGSs? Are the properties of SGSs-I are different from those of SGSs-II? The motivation of the present study is to answer these questions. The rest part of the article is organized as below. Section 2 describes the data analysis. Results and discussion are presented in Section 3. The final section provides the summary.

2. Data and Calculations

2.1. Data Source

High time resolution geomagnetic index used in this study was the SYM-H index, which was obtained from the website at http://wdc.kugi.kyoto-u.ac.jp. The source locations of the SGSs were obtained from the previous articles (e.g., Cliver & Crooker 1993; Zhang et al. 2007; Lefèvre et al. 2016; Vennerstrom et al. 2016; Meng et al. 2019).

2.2. The Calculation of the Properties of an SGS

Because of the data gap for many SGSs, it is difficult to analyze the interplanetary sources of these SGSs. However, the properties of the main phase of an SGS can be acquired from SYM-H index. We use t_s and t_e to indicate the start and the end time of the main phase of an SGS. We use SYM-H$_e$ and SYM-H$_s$ to represent the values of SYM-H index at the moments of t_e and t_s, respectively. The time duration of the main phase is $\Delta t = t_e - t_s$. The variation of SYM-H during the main phase of an SGS is ΔSYM-H, which is calculated as below,

$$\Delta\mathrm{SYM{-}H} = \mathrm{SYM{-}H}_e - \mathrm{SYM{-}H}_s. \tag{1}$$

The averaged increase speed of the ring current during the main phase of an SGS is calculated as below,

$$\Delta\mathrm{SYM{-}H}/\Delta t. \tag{2}$$

Here we give an example to show how to analyze the properties of the main phase of an SGS, which is shown in Figure 1. It is an SGS that occurred on 1989 March 13–14. The first and second red vertical solid lines indicated the start and the end time of the main phase of the SGS. The derived Δt, ΔSYM-H and $|\Delta\mathrm{SYM{-}H}/\Delta t|$ were 1397 min, -790 nT and 0.565 903 nT $\cdot$ minute^{-1}, respectively.

3. Results and Discussion

3.1. The Variation of ΔSYM-H with the Heliolongitudes

There were 24 SGSs from 1981 to 2018. The numbers of SGSs-I and SGSs-II are 16 and 8, respectively. According to the derived Δt, ΔSYM-H and ΔSYM$-$H$/\Delta t$ for each SGS, and according to the source locations of the SGSs, the variation of ΔSYM-H with the heliolongitudes of the SGSs is analyzed and shown in Figure 2. As shown in Figure 2, the source locations of 14 SGSs were distributed in the east hemisphere of the Sun, while the source locations of 10 SGSs were distributed in the west hemisphere of the Sun, indicating that the east hemisphere has more SGSs than the west hemisphere. In addition, the source locations of 23 SGSs were distributed in the longitudinal scope ranging from E40 to W20, indicating that 95.8% of the SGSs were distributed in the longitudinal scope of [E40, W20].

3.2. The Variation of Δt with the Heliolongitude

The variation of Δt with the heliolongitude of the SGSs is shown in Figure 3. We can see from Figure 3 that the durations of the main phases for six SGSs with source locations within the longitudinal area ranging from E15 to W20 varied from 2 to 4 hr. The durations of the main phases for the rest 18 SGSs were longer than 6.5 hr. The duration for the SGSs with source locations in the west hemisphere ranged from 2.22 to 19.583 hr, and the averaged duration of the main phases of these SGSs is 8.3 hr. The duration for the SGSs with source locations in the

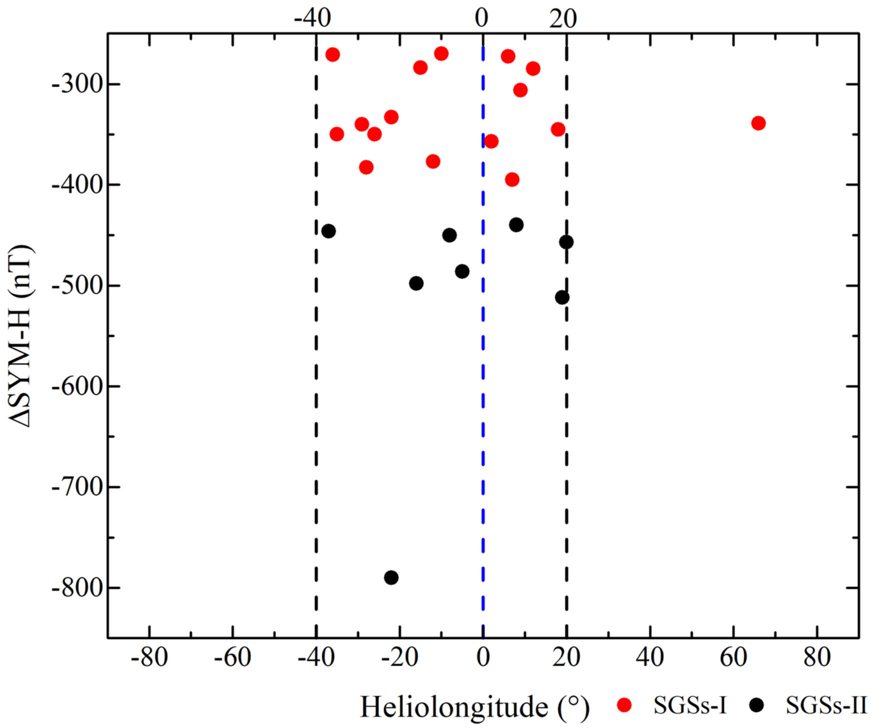

Figure 2. The variation of ΔSYM-H with the heliolongitude.

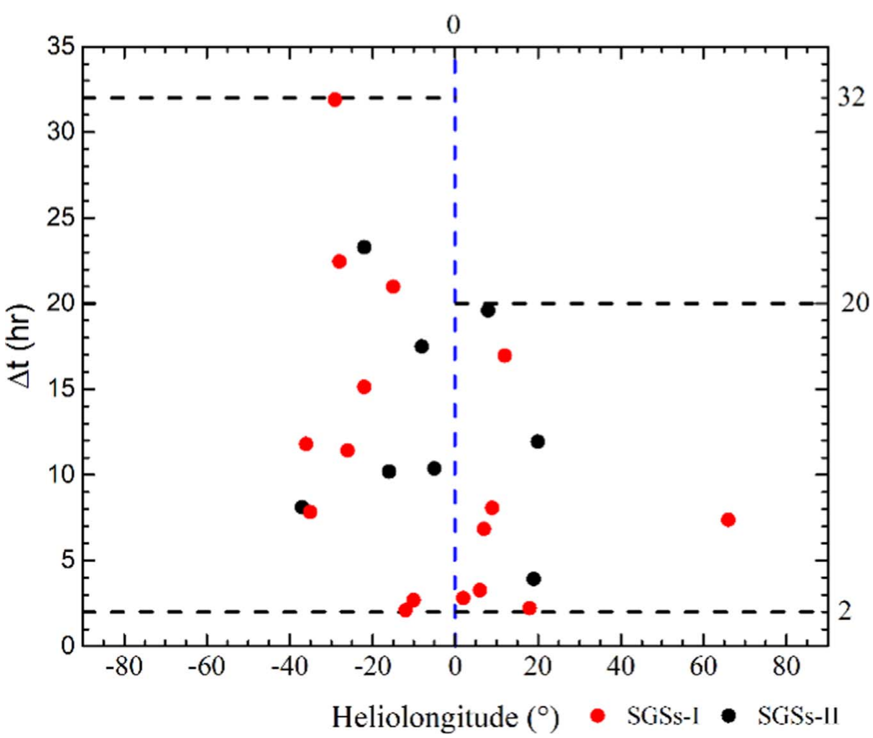

Figure 3. The variation of Δt with the heliolongitude of the SGSs.

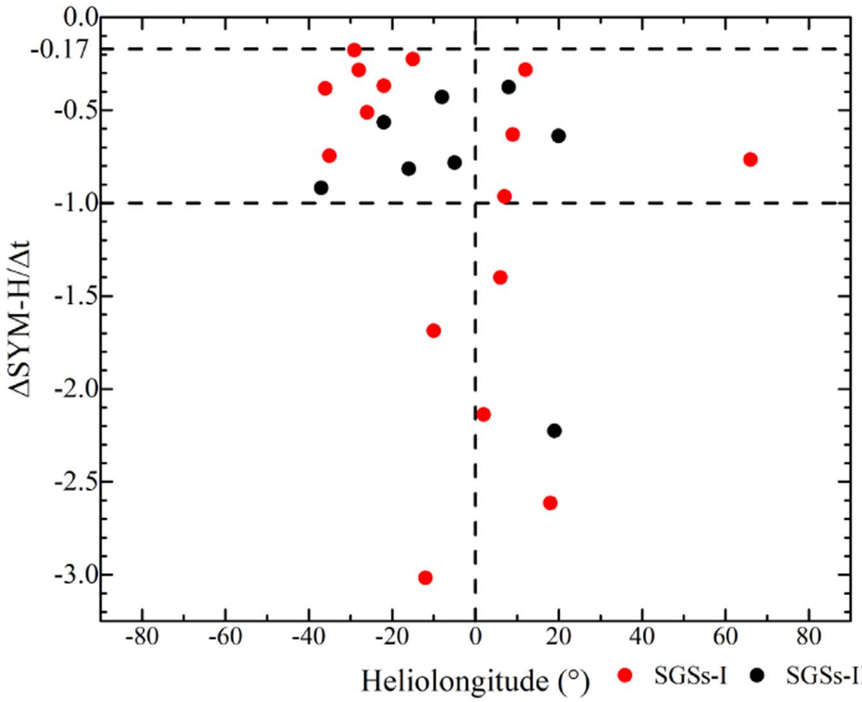

Figure 4. ΔSYM$-$H$/\Delta t$ varied with the heliolongitude of the SGSs.

east hemisphere ranged from 2.1 to 31.88 hr. The averaged duration of the main phases of these SGSs is 13.98 hr.

*3.3. The Variation of ΔSYM−H/Δ*t *with the Heliolongitude*

According to the ΔSYM$-$H$/\Delta t$ of an SGS, the derived ΔSYM$-$H$/\Delta t$ for each SGS is shown in Figure 4. As shown in Figure 4, ΔSYM$-$H$/\Delta t$ for six SGSs was larger than 1.0 nT $\cdot$ minute^{-1}, while ΔSYM$-$H$/\Delta t$ for 18 SGSs was lower than 1.0 nT $\cdot$ minute^{-1}. ΔSYM$-$H$/\Delta t$ for SGSs-II varied from 0.37 to 2.2 nT $\cdot$ minute^{-1}, while ΔSYM$-$H$/\Delta t$ for SGSs-I varied from 0.18 to 3.0 nT $\cdot$ minute^{-1}.

3.4. Discussions

As shown in Figure 5, we use a geomagnetic storm that occurred on 2005 May 15 to explain why we should use the SYM-H index to describe the variation of the ring current of a geomagnetic storm rather than the Dst index. The period between the two vertical red solid lines in the second panel is the main phase of the geomagnetic storm determined by the SYM-H index. The period between the two vertical dashed lines in the top panel is the interplanetary magnetic field responsible for the main phase of the geomagnetic storm described by the SYM-H index. The period between the two vertical blue solid lines in the bottom panel is the main phase of the geomagnetic storm determined by the Dst index. It is easy to judge that, compared with that of the Dst, the evolution of the SYM-H index is much more consistent with that of B_z. This is the reason why we used the SYM-H index to describe the ring current of a geomagnetic storm rather than the Dst index.

The difference between SYM-H$_{\rm min}$ and ΔSYM-H may have different physical meaning, and the difference between SYM-H$_{\rm min}$ and ΔSYM-H may be large. An example shown in Figure 6 is used to explain this. The SYM-H$_{\rm min}$ and ΔSYM-H were -337 nT and -270 nT, respectively, for the SGS on 1989 October 21. The difference between SYM-H$_{\rm min}$ and ΔSYM-H is -67 nT. The reason is that the main phase of the SGS occurred in the recovery phase of a previous geomagnetic storm, leading to the value of the SYM-H index at the start time of the main phase of the SGS much lower than 0 nT. Anyway, the variation of the ring current should be described by ΔSYM-H rather than by SYM-H$_{\rm min}$. Hence, the averaged variation speed of the ring current during the main phase of a geomagnetic storm should be described by ΔSYM$-$H$/\Delta t$ rather than by SYM$-$H$_{\rm min}/\Delta t$. As shown in Figure 6, ΔSYM $-$H$/\Delta t$ was -1.68750 nT $\cdot$ minute^{-1}, indicating that the ring current increased very quickly during the main phase of the SGS.

The geomagnetic storm on 2004 November 10 is shown in Figure 7. The first and the second vertical red solid lines are the start and the end time of the main phase of the geomagnetic storm, respectively. ΔSYM-H was equal to -219 nT, which did not satisfy the condition ΔSYM-H $\leqslant -250$ nT. Therefore,

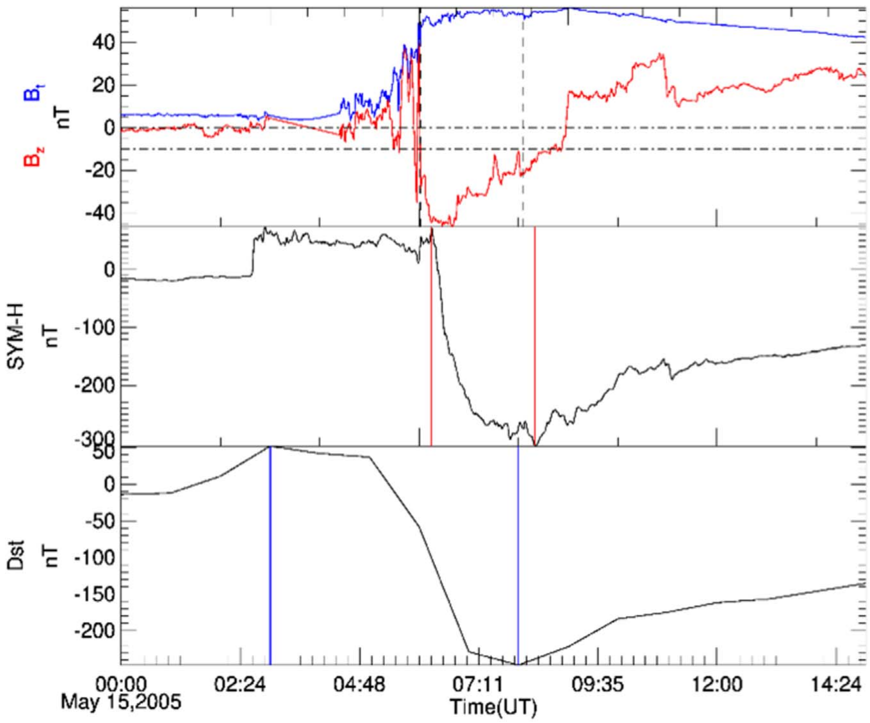

Figure 5. Interplanetary magnetic field (IMF) and the geomagnetic storm on 2005 May 15. From top to bottom, it shows interplanetary magnetic field (blue line for total IMF, red line for z-component of the IMF), SYM-H index and Dst index, respectively. The two horizontal dashed lines in the top panel indicate the zero and -10 nT. The first vertical dashed line indicates the moment 06:01 UT on 2005 May 15 when z-component of IMF started to become minus and decreased continuously. The second vertical dashed line indicates the moment 08:06 UT on 2005 May 15. The first vertical red solid line indicates the moment 06:15 UT on 2005 May 15 when the SYM-H began to decrease continuously. The second vertical red solid line indicates the moment 20:00 UT on 2005 May 15 when the SYM-H reached its minimum value. The first and second vertical blue solid lines in the bottom panel indicate the 03:00 UT and 08:00 UT on 2005 May 15, respectively.

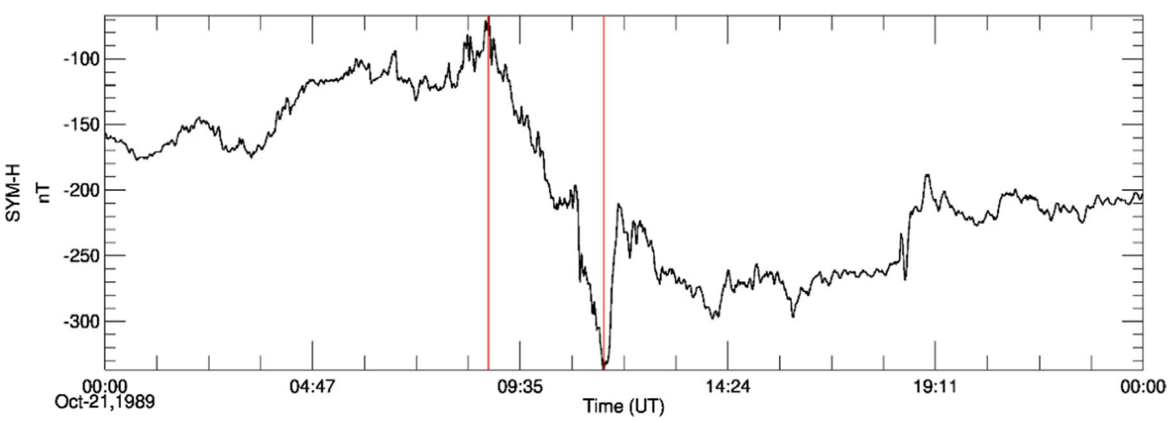

Figure 6. The main phase of the SGS on 1989 October 21.

this storm is not included in the present study although the SYM-H_{min} is -263 nT.

The duration of the main phase of the SGS on 2001 March 31 is 235 minutes, which is the shortest time for the main phases of the SGSs-II. $|\Delta \mathrm{SYM{-}H}/\Delta t|$ for the SGS on 2001 March 31 is nearly 2.23 $\mathrm{nT} \cdot \mathrm{minute}^{-1}$, which is the fastest speed for the SGSs-II. Previous study (Wang et al. 2003a) showed that the SGS on 2001 March 31 was due to the multiple magnetic clouds, which were formed by the overtaking of successive magnetic clouds. Case studies (Cheng et al. 2020; Li et al. 2022; Liu et al. 2022) found that the solar wind density or dynamic pressure played an important role in the ring current

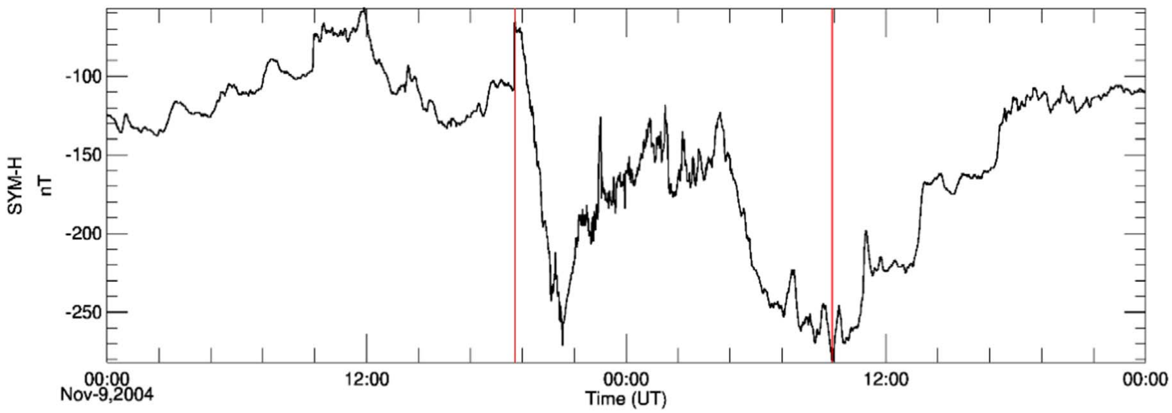

Figure 7. The main phase of the geomagnetic storm on 2004 November 9–10.

increase speed in the SGS on 2001 March 31 and the great geomagnetic storm on 1999 October 21–22. Statistical studies (Le et al. 2020; Zhao et al. 2021; Gopalswamy et al. 2022; Zhao et al. 2022) proved that solar wind dynamic pressure is an important factor for the geomagnetic storm intensity besides the solar wind speed and the southward component (hereafter B_s) of interplanetary magnetic field.

The SGSs-II on 2003 October 29–30, 2003 November 20 and 2004 November 8 were caused by single magnetic cloud (Zhang et al. 2007). The duration of the main phase of the SGS on 2003 October is much longer than those of the two SGSs that occurred on 2003 November 20 and 2004 November 8, respectively, indicating that the properties of the main phase of an SGS not only depend on the corresponding CME properties including the source location and the initial speed of the CME, but also depend on the CME propagation from the Sun to the Earth. We can see from Figure 1 that the main phase of the SGS on 1989 March 13-14 was constituted by multi-step, indicating that the SGS may be caused by successive CMEs. Anyway, the properties of the main phase of a SGS are determined by a variety of factors.

4. Summary

We have studied the properties of the main phases of 24 SGSs with different heilongitudes. According to the above analyses, the results can be summarized as below.

1. Of the 24 SGSs, the number of SGSs-I and SGSs-II were 16 and 8, respectively. 14 SGSs came from the east hemisphere of the Sun and 10 SGSs came from the west hemisphere of the Sun. Source locations of 23 SGSs were distributed in the longitudinal scope ranging from E40 to W20, indicating that 95.8% of the SGSs were distributed in the longitudinal scope of [E40, W20]. The largest SGS came from the east hemisphere of the Sun.
2. The duration of the main phases for six SGSs, with source locations distributed in the longitudinal area scope of [E15, W20], was 2–4 hr. The durations of the main phases for the rest 18 SGSs were longer than 6.5 hr. The duration of the SGSs with source locations in the west hemisphere ranged from 2.22 to 19.583 hr, and the averaged duration of the main phases of these SGSs is 8.3 hr. The duration for the SGSs with source locations in the east hemisphere ranged from 2.1 to 31.88 hr. The averaged duration of the main phases of these SGSs is 13.98 hr.
3. $|\Delta\mathrm{SYM{-}H}/\Delta t|$ for six SGSs with source locations distributed in the longitudinal area ranging from E15 to W20 was larger than $1.0\,\mathrm{nT}\cdot\mathrm{minute}^{-1}$, while $|\Delta\mathrm{SYM{-}H}/\Delta t|$ for the rest 18 SGSs was lower than $1.0\,\mathrm{nT}\cdot\mathrm{minute}^{-1}$. $|\Delta\mathrm{SYM{-}H}/\Delta t|$ for SGSs-II varied from 0.37 to $2.2\,\mathrm{nT}\cdot\mathrm{minute}^{-1}$, while $|\Delta\mathrm{SYM{-}H}/\Delta t|$ for SGSs-I varied from 0.18 to $3.0\,\mathrm{nT}\cdot\mathrm{minute}^{-1}$.

Acknowledgments

We acknowledge the use of NASA and GSFCs Space Physics Data Facilitys OMNI data and web service (https://omniweb.gsfc.nasa.gov/html/omni_min_data.html). The geomagnetic field data used in this paper were provided by the WDC for Geomagnetism, Kyoto (http://wdc.kugi.kyoto-u.ac.jp/wdc/Sec3.html). This research was funded by the Sino-South Africa Joint Research on Polar Space Environment (2021YFE0106400), International Cooperation Project on Scientific and Technological Innovation Between Governments, National Key Plans on Research and Development, Ministry of Science and Technology, China, the Special Fund of the Institute of Geophysics, China Earthquake Administration (Grant No. DQJB21X26), CAS Key Laboratory of Solar Activity under No. KLSA202109, and the National Natural Science Foundation of China (Grant Nos. 41074132, 41474166, 41774195 and 41774085).

ORCID iDs

Ming-Xian Zhao https://orcidorg/0000-0002-1031-018X
Gui-Ming Le https://orcidorg/0000-0002-9906-5132

References

Allen, J., Sauer, H., Frank, L., & Reiff, P. 1989, Eos, Trans. Am. Geophys. Union, 70, 1479
Burton, R. K., McPherron, R. L., & Russell, C. T. 1975, JGR, 80, 4204
Cheng, L.-B., Le, G.-M., & Zhao, M.-X. 2020, RAA, 20, 036
Cliver, E. W., Balasubramaniam, K. S., Nitta, N. V., & Li, X. 2009, JGRA, 114, A00A20
Cliver, E. W., & Crooker, N. U. 1993, SoPh, 145, 347
Cliver, E. W., Schrijver, C. J., Shibata, K., & Usoskin, I. G. 2022, LRSP, 19, 2
Council National Research 2008, SpWea Events: Understanding Societal and Economic Impacts: A Workshop Report (Washington, DC: National Academies Press),
Eastwood, J. P., Biffis, E., Hapgood, M. A., et al. 2017, Risk Anal., 37, 206
Farrugia, C. J., Matsui, H., Kucharek, H., et al. 2005, JGRA, 110, A09S13
Fenrich, F. R., & Luhmann, J. G. 1998, GeoRL, 25, 2999
Ganushkina, N., Jaynes, A., & Liemohn, M. 2017, SSRv, 212, 1315
Garcia, H. A., & Dryer, M. 1987, SoPh, 109, 119
Gopalswamy, N. 2018, in Extreme Events in Geospace, ed. N. Buzulukova (Amsterdam: Elsevier), 37
Gopalswamy, N., Yashiro, S., Akiyama, S., et al. 2022, JGRA, 127, e2022JA030404
Gopalswamy, N., Yashiro, S., Liu, Y., et al. 2005a, JGRA, 110, A09S15
Gopalswamy, N., Yashiro, S., Michalek, G., et al. 2005b, GeoRL, 32, L12S09
Huttunen, K. E. J., Koskinen, H. E. J., Pulkkinen, T. I., et al. 2002, JGRA, 107, 1440
Jadav, R., Iyer, K., Joshi, H., & Vats, H. O. 2005, P&SS, 53, 671
Kataoka, R., & Miyoshi, Y. 2008, GeoRL, 35, L06S09
Katus, R. M., & Liemohn, M. W. 2013, JGRA, 118, 5149
Kumar, S., Veenadhari, B., Tulasi Ram, S., et al. 2015, JGRA, 120, 7307
Le, G.-M., Liu, G.-A., & Zhao, M.-X. 2020, SoPh, 295, 108
Le, G.-M., Zhao, M.-X., & Q.-L. 2021a, MNRAS, 502, 2043
Le, G.-M., Zhao, M.-X., Zhang, W.-T., & Liu, G.-A. 2021b, SoPh, 296, 187
Lefèvre, L., Vennerstrøm, S., Dumbović, M., et al. 2016, SoPh, 291, 1483
Li, Q., Zhao, M.-X., & Le, G.-M. 2022, Univ, 8, 346
Liu, G.-A., Zhao, M.-X., Le, G.-M., et al. 2022, RAA, 22, 015002
Liu, Y. D., Luhmann, J. G., Kajdič, P., et al. 2014, NatCo, 5, 3481
Love, J. J. 2021, SpWea, 19, e2020SW002579
Lugaz, N., Farrugia, C. J., Huang, C.-L., & Spence, H. E. 2015, GeoRL, 42, 4694
Meng, X., Tsurutani, B. T., & Mannucci, A. J. 2019, JGRA, 124, 3926
Murayama, T. 1982, RvGeo, 20, 623
O'Brien, T. P., & McPherron, R. L. 2000, JGRA, 105, 7707
Riley, P., Baker, D., Liu, Y. D., et al. 2018, SSRv, 214, 21
Riley, P., & Love, J. J. 2017, SpWea, 15, 53
Schulte in den Bäumen, H., Moran, D., Lenzen, M., Cairns, I., & Steenge, A. 2014, NHESS, 14, 2749
Smart, D. F., & Shea, M. A. 1996, AdSpR, 17, 147
Temerin, M., & Li, X. 2002, JGRA, 107, 1472
Tsurutani, B. T., Gonzalez, W. D., Lakhina, G. S., & Alex, S. 2003, JGRA, 108, 1268
Vennerstrom, S., Lefevre, L., Dumbović, M., et al. 2016, SoPh, 291, 1447
Wang, Y., Shen, C. L., Wang, S., & Ye, P. Z. 2003b, GeoRL, 30, 2039
Wang, Y. M., Ye, P. Z., & Wang, S. 2003a, JGRA, 108, 1370
Wanliss, J. A., & Showalter, K. M. 2006, JGRA, 111, A02202
Wu, C. -C., Liou, K., Lepping, R. P., et al. 2016, EP&S, 68, 151
Xue, X., Wang, Y., Ye, P., Wang, S., & Xiong, M. 2005, P&SS, 53, 443
Zhang, J., Richardson, I. G., Webb, D. F., et al. 2007, JGRA, 112, A10102
Zhao, M.-X., Le, G.-M., Li, Q., Liu, G.-A., & Mao, T. 2021, SoPh, 296, 66
Zhao, M.-X., Le, G.-M., & Lu, J. 2022, ApJ, 928, 18